

Contact-mediated signaling enables disorder-driven transitions in cellular assemblies

Chandrashekar Kuyyamudi,^{1,2} Shakti N. Menon,¹ and Sitabhra Sinha^{1,2}

¹The Institute of Mathematical Sciences, CIT Campus, Taramani, Chennai 600113, India

²Homi Bhabha National Institute, Training School Complex, Anushaktinagar, Mumbai 400 094, India

(Dated: January 19, 2022)

We show that when cells communicate by contact-mediated interactions, heterogeneity in cell shapes and sizes leads to qualitatively distinct collective behavior in the tissue. For inter-cellular coupling that implements lateral inhibition, such disorder-driven transitions can substantially alter the asymptotic pattern of differentiated cells by modulating their fate choice through changes in the neighborhood geometry. In addition, when contact-induced signals influence inherent cellular oscillations, disorder leads to the emergence of functionally relevant partially-ordered dynamical states.

Many natural systems, ranging from granular materials to biological tissues and dense crowds, are characterized by varying levels of heterogeneity in their structural attributes [1–6]. This disorder arises via self-organization as a result of interactions between their numerous constituent units, causing their arrangement to deviate from regular lattice ordering [7–10]. A striking example in the biological context is provided by confluent epithelial tissue, whose constituent cells are packed together in a high state of disorder, as characterized by quantitative measures that incorporate the area, perimeter or number of neighbors of each cell [11–13]. Moreover, as the cells communicate with each other, e.g., via the ubiquitous Notch pathway in which signaling occurs via receptor-ligand binding [14–16], disorder may also have remarkable functional consequences. Note that the Notch pathway effectively implements *lateral inhibition* through which the induction of a specific fate in a particular cell prevents its immediate neighbors from expressing the same fate [17, 18]. As this is one of the principal mechanisms through which patterning arises in tissues [19, 20], any disorder in the geometry of neighborhood contacts that alter the nature of interactions between adjacent cells consequently affects their fates [21]. A natural question in this context relates to the relative roles of local, contact-mediated interactions and global forces that alter the degree of disorder in shaping the collective behavior of cellular assemblies.

A striking illustration of such interplay between disorder and interactions can be seen during the appearance of a characteristic spatial pattern of cells in the basal papilla (the auditory sensory organ in all amniotes [22]), comprising specialized sensory “hair cells” that are separated from each other by intervening support cells [Fig. 1 (a)]. As either cell type can arise from the same progenitor cell, the specific fate induced in a particular cell depends on the cues it receives from its neighborhood [23]. In particular, hair cells inhibit their immediate neighbors from adopting the same fate [17, 24]. Disorder in the structural arrangement of a cell’s neighborhood can drastically affect these cues and consequently, the resulting fate choice. More generally, one can investigate novel

qualitative features in the collective behavior, such as partially ordered or “chimera” states [25, 26], that may result from structural heterogeneities. This is particularly relevant where heterogeneity arises through flexibility in cell shapes, typically observed at the embryonic stage [27] but retained lifelong in simpler animals such as *Trichoplax adhaerens* [28]. The resulting disordered arrangement of cells in this organism, when coupled to the oscillatory dynamics of the cilia of each cell, can affect organism-level behavior such as gliding locomotion along surfaces propelled by collective beating of the cilia [29, 30] [Fig. 1 (b)]. These examples suggest that the composition and function of tissues can be altered significantly with increasing heterogeneity in cell sizes and shapes.

In this paper we explicitly demonstrate such transitions with increasing disorder in the arrangement of cells that interact via contact-induced signaling. When the interactions between cells implement lateral inhibition, it can influence fate induction to alter the relative proportions of distinct cell types, and consequently affect development. We also demonstrate that in tissues where cells are susceptible to random failures in their ability to communicate with neighbors, heterogeneity in the cellular packing geometry makes the asymptotic pattern of differentiated cells more robust. Further, if the inter-cellular interactions modulate activity in the cells, such as oscillations in molecular concentrations [31–34], we observe that disorder promotes the emergence of the complex spatio-temporal phenomenon of chimera states. These are characterized by the coexistence of oscillating cells with those whose activity has been arrested, and we show that they arise irrespective of whether adjacent cells are coupled through receptor-ligand binding or by diffusion across bridges such as gap junctions [Fig. 1 (c-e)]. Thus, selective deformation of a cellular assembly can drive transitions between dynamical states marked by different proportions of oscillating elements, suggesting an intriguing locomotory mechanism in simple multicellular organisms.

To generate disordered cellular configurations we use the method of Voronoi tessellations to construct two-dimensional space-filling tilings with non-overlapping

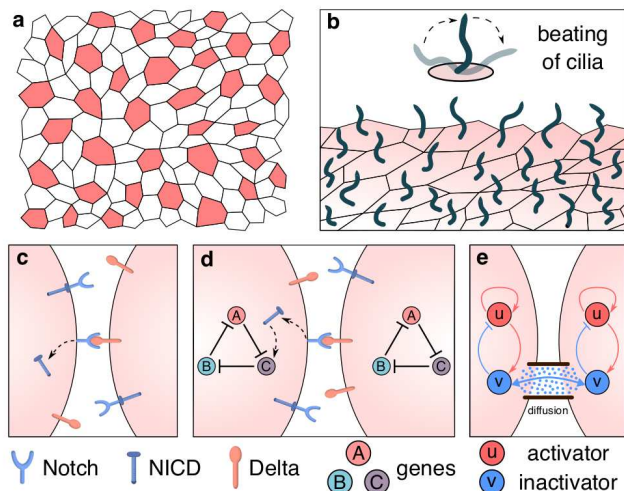


FIG. 1. **Communication between neighboring cells in a close-packed disordered configuration underlie a range of collective behavior.** (a) Schematic diagram of the spatial arrangement of hair cells (shown in red) surrounded by supporting cells in the avian basilar papilla, at an early stage of development [23]. (b) Ventral tissue of the marine animal *Trichoplax adhaerens* illustrated schematically to show the arrangement of monociliated epithelial cells [35–37]. Each of the cilia engage in periodic motion (“beating”, see inset) that helps propel the organism across a surface [29, 30]. (c-e) The key qualitative features of the collective dynamics in such systems are seen to be invariant despite differences in the means by which cells communicate and the dynamics within each cell, e.g., in cells coupled via *trans*-activation of Notch receptors by Delta ligands resulting in release of a downstream effector (NICD) [shown in (c)], repressilators coupled by Notch-Delta signaling (d) and relaxation oscillators coupled via diffusion of the inactivation variable through inter-cellular bridges such as gap junctions (e).

polygons that are characterized by varying levels of heterogeneity. We begin with a regular hexagonal lattice that is then disordered by adding Gaussian noise $\mathcal{N}(0, \sigma_P)$ to randomly displace each of the generating points or seeds (initially, the centroids of the hexagons). The standard deviation σ_P can be tuned to yield different levels of heterogeneity. The extent of disorder in the lattice, measured by the variance of the perimeters of the cellular polygons $\sigma^2(l_e)$, reaches its maximal value for $\sigma_P \sim 1$ and does not change appreciably on increasing σ_P further [Fig. 2]. The strength of coupling between a pair of adjacent cells is assumed to be proportional to the total length of their interface. A weighted adjacency matrix \mathbf{A} , with A_{ij} representing the overlap between the cells i and j , thus provides the information required to assign interaction strengths between each pair of cells.

We consider contact-induced signaling via Notch receptors located on the surface of a cell binding to ligands (e.g., Delta) embedded in the membrane of a neighboring cell (i.e., *trans* binding). This is represented by the

following set of equations describing the time-evolutions of the concentrations of the receptor (R), ligand (L) and the Notch intra-cellular domain or NICD (S), the downstream effector of the Notch signaling pathway:

$$\frac{dR_i}{dt} = \beta_R - \gamma_R R_i - k_{cis} R_i L_i - k_{tr} R_i L_i^{tr}, \quad (1)$$

$$\frac{dL_i}{dt} = \frac{\beta_L K_s^h}{K_s^h + S_i^h} - \gamma_L L_i - k_{cis} R_i L_i - k_{tr} L_i R_i^{tr}, \quad (2)$$

$$\frac{dS_i}{dt} = k_{tr} R_i L_i^{tr} - \gamma_S S_i. \quad (3)$$

Here $R_i^{tr} = \sum_j A_{ij} R_j$ and $L_i^{tr} = \sum_j A_{ij} L_j$ are the weighted sums of receptor and ligand concentrations, respectively, in the neighborhood of the i^{th} cell. Earlier studies have shown that lateral inhibition requires strong inhibition of Notch receptors via *cis* binding (i.e., to ligands on the same cell) [17, 18]. Consistent with this, we choose $k_{tr} = 0.13$ and $k_{cis} = 4.64$, which are related to the rates of *trans* activation and *cis* inhibition, respectively. The maximal production rates of both receptors (β_R) and ligands (β_D) are chosen to be 100. The contact-induced signal is assumed to have a relatively longer lifetime so that the degradation rates of the receptors (γ_R), ligands (γ_D) and NICD (γ_S) are chosen as 1, 1 and 0.1, respectively. The repression of ligand production by the downstream effector of Notch signaling pathway is modeled by a Hill function, parameterized by $K_s (= 10)$ and $h (= 4)$. The initial concentrations for the ligands and receptors are chosen from a uniform random distribution defined over the domain $[0, 10]$.

In presence of strong *cis* inhibition, only those cells in which ligands far outnumber receptors can engage in *trans* activation of Notch receptors of neighboring cells. Consequently, the production of ligands in these cells is inhibited [see Eqn. (2)]. The resulting unequal distribution of ligands among cells results in each of them eventually becoming either (i) a *receiver* cell having receptors but no ligands, such that it can only “receive” contact-induced inter-cellular signals, or (ii) a *transmitter* cell, which possess ligands but no receptors, such that it can only “send out” signals. Mutual competition for *trans*-binding between neighboring cells having more ligands than receptors is reinforced by the suppression of ligand production in the cell whose receptors are activated. Thus, each cell which develops into a transmitter would be surrounded exclusively by cells which adopt the fate of receivers [17]. This mutual “repulsion” between transmitter cells imposes a strong constraint on their numbers as such cells need to be separated from each other by receiver cells. For example, this requirement would allow only $\sim N/3$ transmitters in a hexagonal lattice comprising N cells. However, instead of a regular lattice, if we consider a disordered arrangement, e.g., a sheet of epithelial cells, the total number of transmitter cells allowed in the resulting packing increases noticeably [38]. This can be observed from Fig. 2 (a) which shows the spatial pat-

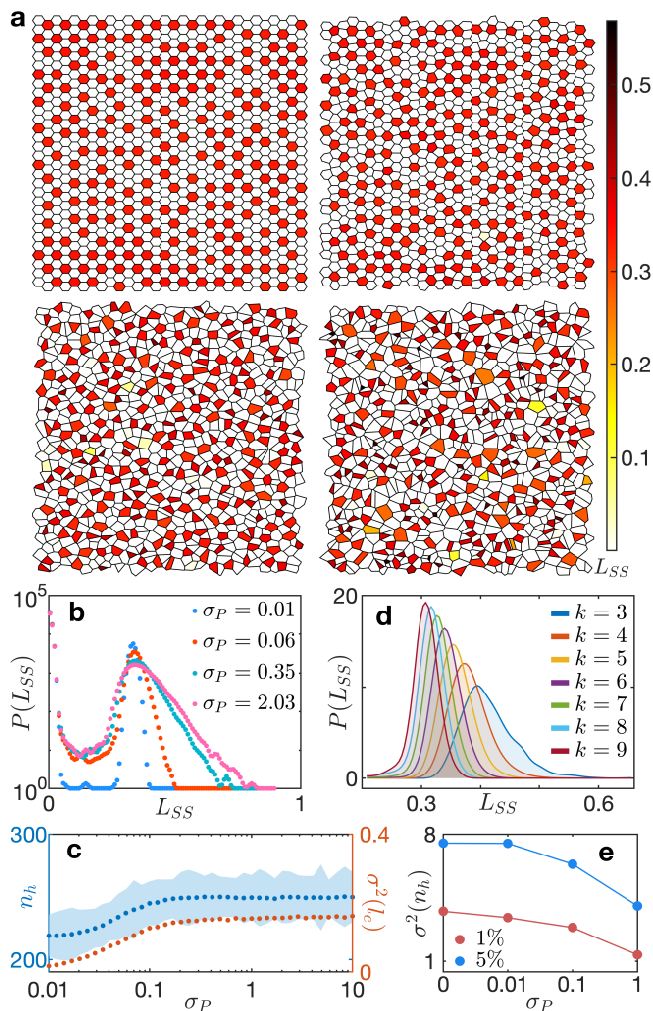


FIG. 2. Higher disorder in the cellular packing configuration allows a more equitable and robust distribution of cell fates. (a) Spatial patterns formed by the steady state Delta ligand concentration, L_{SS} (see color bar) in an assembly of $N(= 900)$ cells resulting from lateral inhibition. The panels represent increasingly disordered configurations as indicated by the dispersion of the deviations in cell positions from those in the regular hexagonal lattice: $\sigma_P = 0$ (top left), 0.01 (top right), 0.1 (bottom left) and 1 (bottom right). As seen from the bimodal distribution in (b), cells either have very low or high values of L_{SS} . The increase in the width of the high L_{SS} peak with disorder is quantified in (c) which shows that the number of cells n_h (blue dots) in this state increases with the disorder [50]. The shaded region represents the dispersion in n_h . The variance of the cell perimeters ($\sigma^2(l_c)$, red dots) also rises with disorder in a qualitatively similar manner. (d) The asymptotic ligand concentration in a cell appears to be correlated with the number of its neighbors k . The L_{SS} distributions in cells with a specific k monotonically shift to left with increasing k , suggesting that cells in states characterized by higher L_{SS} have fewer neighbors than average. (e) Greater robustness to damage in the cellular array is seen with increased disorder, as evident from the reduced variability of fate distribution (measured in terms of dispersion in n_h) with rise in σ_P when 1% (red) or 5% (blue) of randomly chosen cells are rendered inert.

terms of cellular ligand concentration L_{SS} in the steady state as σ_P is increased.

The observed bimodal nature of the L_{SS} distribution is invariant to disorder [Fig. 2 (b)]. Such a distribution allows a natural segregation of the cells into receivers and transmitters, corresponding to populations around its lower and higher peaks, respectively. Further, we note that the cell-cell interface lengths, which crucially dictate the magnitude of the contact-induced signal, exhibit higher variance with increased disorder [Fig. 2 (c)]. This is mirrored in the rise of the number of transmitter cells n_h with σ_P [Fig. 2 (c)]. The broadening of the peaks in the L_{SS} distribution with increasing heterogeneity of the cellular configuration can be understood in terms of the role that the degree k of a transmitter cell (i.e., the number of cells in its immediate neighborhood) plays in determining the steady state ligand concentration. Fig. 2 (d) shows that the ligand distribution of cells having exactly k neighbors shifts to the right with decreasing k . Thus, the peak-broadening with σ_P [Fig. 2 (b)] can be attributed to a higher density of transmitter cells with lower k (compared to the regular lattice). With increasing heterogeneity, transmitter cells have fewer neighbors on average, implying that more cells can become transmitters as their number is only limited by the constraint that no two of them can be neighbors.

As transmitters and receivers correspond to cells with distinct fates, the change in the relative proportion of such cells resulting from disordered cellular arrangements suggests that this can alter the course of development. Heterogeneity also makes the spatial pattern robust against damage that may strike a cell at random, disabling it from taking part in inter-cellular signaling [51]. This is quantified by the dispersion in n_h , the number of cells likely to become transmitters, shown in Fig. 2 (e) for two different fractions of randomly damaged cells. As σ_P is increased, the variance decreases noticeably, suggesting that more disordered cellular configurations have less variability in terms of the relative proportion of cells having distinct fates.

The model system reported above focuses only on signaling between cells, without considering how such signals can alter the intra-cellular dynamics. However, Notch signaling is known to play an important role in processes such as somitogenesis [40, 41] and tissue growth by cell division [42, 43], where it takes part in non-trivial dynamics, involving periodically varying molecular concentrations. Therefore, we now consider cellular dynamics described by an oscillating circuit comprising three cyclically repressing genes A , B and C [44], any one of which is assumed to be regulated by the inter-cellular signal S . The collective dynamics of these cellular oscillators coupled by Notch signaling (specifically, by S inhibiting C) can be described by the time-evolutions of R , L and S described earlier (with $h = 2$, other parameter values unchanged), augmented by the following equations for the

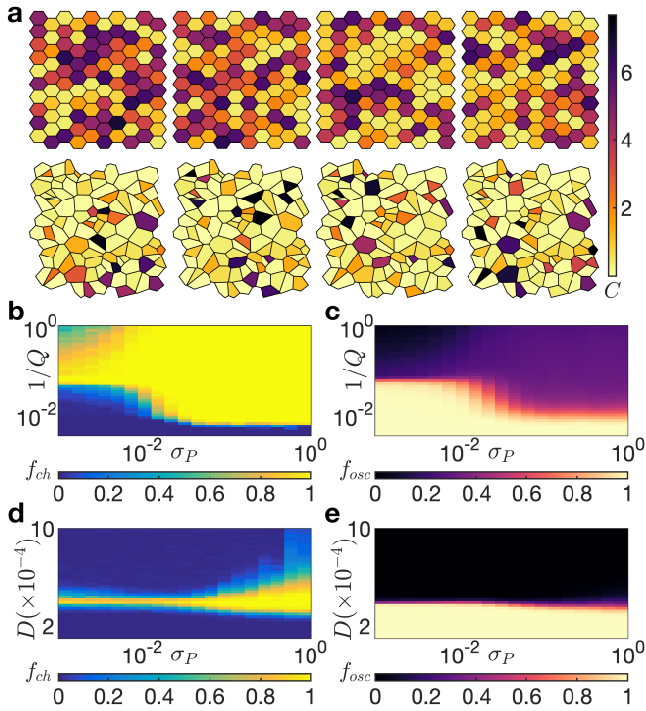


FIG. 3. Disorder promotes the coexistence of qualitatively distinct behaviors (chimera states) in the collective dynamics of cellular oscillators coupled via contact-mediated interactions. (a) Instantaneous states of oscillator arrays that are (top row) ordered ($\sigma_P = 0$), or (bottom row) disordered to the maximum extent ($\sigma_P = 1$), shown at times separated by an interval that is $1/4$ of the oscillation period of an uncoupled cell. Colors represent the expression level of one of the genes (C) comprising the oscillating repressor circuit [39]. (b-c) The fraction of realizations f_{ch} in which chimera states are observed (b) and the mean fraction of cells that continue to oscillate f_{osc} (c) shown as a function of the disorder in cellular arrangement (σ_P), as well as the strength of inter-cellular interaction induced repression (measured as $1/Q$). (d-e) Qualitatively similar behaviors in (d) f_{ch} and (e) f_{osc} are shown by systems of diffusively coupled relaxation oscillators. Increasing the diffusion constant D beyond a critical value leads to cessation of activity through oscillator death. In both systems, increased disorder allows configurations with coexisting oscillating and non-oscillating cells to exist over a much larger range.

gene products:

$$\begin{aligned} \frac{dA_i}{dt} &= \alpha \left[\frac{K^g}{K^g + C_i^g} \right] - \frac{A_i}{\tau}, \\ \frac{dB_i}{dt} &= \alpha \left[\frac{K^g}{K^g + A_i^g} \right] - \frac{B_i}{\tau}, \\ \frac{dC_i}{dt} &= \alpha \left[\frac{K^g}{K^g + B_i^g} \right] \left[\frac{Q^g}{Q^g + S_i^g} \right] - \frac{C_i}{\tau}. \end{aligned}$$

The maximal production rates $\alpha (= 10)$, mean lifetimes $\tau (= 1)$, and the parameters $K (= 1)$ and $g (= 4)$ of the Hill functions describing the cyclic repression are chosen to ensure oscillations in absence of inter-cellular coupling.

The repression of gene expression by S is also modeled by a Hill function, parameterized by the exponent $g (= 4)$ and the half-saturation constant Q . Upon strengthening the repression (i.e., increasing $1/Q$), the collective dynamics shows a transition from global oscillations to a quiescent state that arises from oscillation arrest. Introducing disorder in the cellular arrangement leads to the emergence of chimera states in the collective dynamics [Fig. 3 (a)]. Depending on the context, such states have diverse implications, e.g., in growing tissues characterized by coupled cell-cycle oscillations, they potentially contribute to morphogenesis by selective growth, as only the cells that continue to oscillate can keep dividing [21]. Chimera states could also shape the trajectory of an organism whose locomotion is guided by oscillatory beating of ciliary rotors [as in *T. adhaerens*, Fig. 1 (b)] by selectively rendering certain cilia immotile. As heterogeneity is increased, the range of coupling strengths for which chimera states can be observed increases markedly, appearing even for very weak interactions between cells [Fig. 3 (b)]. This is accompanied by cessation of oscillations in the majority of the cells even at low levels of repression [$Q \sim 10^2$, see Fig. 3 (c)].

The generality of these results can be demonstrated by using a generic description of relaxation oscillations to describe the dynamical behavior of each cell. This involves a fast activation component u and a relatively slower inactivation (or inhibitory) variable v , whose time-evolution is given by the Fitzhugh-Nagumo equations [45–47]. The lateral inhibition resulting from the receptor-ligand binding mediated interaction mechanism is implemented by diffusive coupling via v between the oscillators [48, 49], viz., $du_i/dt = u_i(1 - u_i)(u_i - \phi) - v_i$, $dv_i/dt = \epsilon(\kappa u - v - b) + D \sum_j A_{ij}(v_j - v_i)$, where \mathbf{A} is the weighted adjacency matrix. The parameters $\phi (= 0.139)$, $b (= 0.17)$ and $\kappa (= 0.6)$ specify the kinetics, and $\epsilon (= 0.001)$ is the recovery rate. The strength of diffusive coupling D between neighboring oscillators, which is the analog of the parameter $1/Q$ for the system of coupled repressors, is altered systematically in our simulations. Note that, increasing disorder in the cellular arrangement alters the diffusive flux between coupled cells, which is proportional to the length of the corresponding interface. This is consistent with the linear extent of the cellular interface being proportional to the density of gap junctions (or other structures that bridge the cytoplasm of cells), provided that they are homogeneously distributed across the cell membrane. Fig. 3 (d) shows that, as in the case of Notch coupled repressors, increasing heterogeneity promotes the existence of chimera states over a range of D [51]. They can be characterized by the fraction of oscillating cells f_{osc} lying between 0 and 1, with the chimera region straddling the boundary separating global synchronization ($f_{osc} = 1$) from complete quiescence ($f_{osc} = 0$) [Fig. 3 (e)]. We have verified that the qualitative features of the transition remain invariant to

stochastic fluctuations in molecular concentrations [51]. Thus, disorder-driven transitions appear to be a general phenomenon that might be observed in systems with different mechanisms for oscillations and diverse types of inter-cellular interactions.

To conclude, we have shown that changes in the packing arrangement of cells, as they become more heterogeneous, modulate their collective behavior arising from inter-cellular interactions implementing lateral inhibition. This can play a key role in determining the relative proportions of specialized cells, such as those expressing thoracic bristles in *Drosophila* [24, 52] or neurons that arise by selective differentiation of progenitor cells in the mammalian nervous system [53]. Furthermore, disorder contributes to the robustness of the specific composition of tissues to cell damage. The promotion of chimera states in the collective dynamics of cells upon increasing their heterogeneity has multiple implications, including providing a mechanism for selective regulation of growth in confluent tissue or establishing left-right asymmetry by altering large-scale patterns in ciliary motion during development [54]. Our results can be experimentally corroborated in epithelial sheets of cells interacting via contact-mediated coupling and characterized by varying degrees of disorder. For example, *T. adhaerens* whose cells are capable of continually, and radically, altering their shape [28, 55], can provide a test-bed for relating disordered configurations of epithelial tissue with the collective motion of the cilia attached to every cell. Biofilms comprising oscillating bacterial cells that coordinate their activity by electrical signaling can be another potential experimental system to explore how disordered arrangements alter collective dynamics [56, 57]. Further work may also elucidate the potential role of disorder, which arises naturally via cellular remodeling during development, in shaping morphogenesis.

SNM has been supported by the IMSc Complex Systems Project (12th Plan), and the Center of Excellence in Complex Systems and Data Science, both funded by the Department of Atomic Energy, Government of India. The simulations required for this work were performed using the IMSc High Performance Computing facility (hpc.imsc.res.in) [Nandadevi].

-
- [1] H. M. Jaeger and S. R. Nagel, *Science* **255**, 1523 (1992). doi:10.1126/science.255.5051.1523
- [2] H. M. Jaeger, S. R. Nagel, and R. P. Behringer, *Rev. Mod. Phys.* **68**, 1259 (1996). doi:10.1103/RevModPhys.68.1259
- [3] W. T. Gibson and M. C. Gibson, *Curr. Top. Dev. Biol.* **89**, 87 (2009). doi:10.1016/S0070-2153(09)89004-2
- [4] X. Trepast and E. Sahai, *Nat. Phys.* **14**, 671 (2018). doi:10.1038/s41567-018-0194-9
- [5] A. Bottinelli, D. T. Sumpter, and J. L. Silver-

- berg, *Phys. Rev. Lett.* **117**, 228301 (2016). doi:10.1103/PhysRevLett.117.228301
- [6] A. Kulkarni, S. P. Thampi, and M. V. Panchagnula, *Phys. Rev. Lett.* **122**, 048002 (2019) doi:10.1103/PhysRevLett.122.048002
- [7] T. Lecuit and P.-F. Lenne, *Nat. Rev. Mol. Cell Bio.* **8**, 633 (2007). doi:10.1038/nrm2222
- [8] G. B. Blanchard, A. J. Kabla, N. L. Schultz, L. C. Butler, B. Sanson, N. Gorfinkiel, L. Mahadevan, and R. J. Adams, *Nat. Methods* **6**, 458 (2009). doi:10.1038/nmeth.1327
- [9] F. Jülicher and S. Eaton, *Semin. Cell Dev. Biol.* **67**, 103 (2017). doi:10.1016/j.semcdb.2017.04.004
- [10] K. Molnar and M. Labouesse, *Open Biol.* **11**, 210006 (2021). doi:10.1098/rsob.210006
- [11] J. A. Zallen and R. Zallen, *J. Phys. Condens. Mat.* **16**, S5073 (2004). doi:10.1088/0953-8984/16/44/005
- [12] S. Hilgenfeldt, S. Erisken, and R. W. Carthew, *Proc. Natl. Acad. Sci. USA* **105**, 907 (2008). doi:10.1073/pnas.0711077105
- [13] K. Ragkousi and M. C. Gibson, *J. Cell Biol.* **207**, 181 (2014). doi:10.1083/jcb.201408044
- [14] S. Artavanis-Tsakonas, K. Matsuno, and M. E. Fortini, *Science* **268**, 225 (1995). doi:10.1126/science.7716513
- [15] R. Kopan and M. X. G. Ilagan, *Cell* **137**, 216 (2009). doi:10.1016/j.cell.2009.03.045
- [16] D. Sprinzak, A. Lakhanpal, L. LeBon, J. Garcia-Ojalvo, and M. B. Elowitz, *PLoS Comput. Biol.* **7**, e1002069 (2011). doi:10.1371/journal.pcbi.1002069
- [17] O. Barad, D. Rosin, E. Hornstein, and N. Barkai, *Sci. Signal.* **3**, ra51 (2010). doi:10.1126/scisignal.2000857
- [18] D. Sprinzak, A. Lakhanpal, L. LeBon, L. A. Santat, M. E. Fontes, G. A. Anderson, J. Garcia-Ojalvo, and M. B. Elowitz, *Nature (London)* **465**, 86 (2010). doi:10.1038/nature08959
- [19] H. Meinhardt and A. Gierer, *J. Cell Sci.* **15**, 321 (1974). doi:10.1242/jcs.15.2.321
- [20] L. Wolpert and C. Tickle, *Developmental Biology* (Oxford University Press, Oxford, 2011).
- [21] C. Kuyyamudi, S. N. Menon, F. Casares, and S. Sinha, *Phys. Rev. E* **104**, L052401 (2021). doi:10.1103/PhysRevE.104.L052401
- [22] B. Fritzsche, N. Pan, I. Jahan, J. S. Duncan, B. J. Kopecky, K. L. Elliott, J. Kersigo, and T. Yang, *Evol. Dev.* **15**, 63 (2013). doi:10.1111/ede.12015
- [23] R. Goodyear and G. Richardson, *J. Neurosci.* **17**, 6289 (1997). doi:10.1523/JNEUROSCI.17-16-06289.1997
- [24] P. Simpson, *Development* **109**, 509 (1990). doi:10.1242/dev.109.3.509
- [25] D. M. Abrams and S. H. Strogatz, *Phys. Rev. Lett.* **93**, 174102 (2004). doi:10.1103/PhysRevLett.93.174102
- [26] R. Singh, S. Dasgupta, and S. Sinha, *Europhys. Lett.* **95**, 10004 (2011). doi:10.1209/0295-5075/95/10004
- [27] S. Kim, M. Pochitaloff, G. A. Stooke-Vaughan, and O. Campàs, *Nat. Phys.* **17**, 859 (2021). doi:10.1038/s41567-021-01215-1
- [28] V. N. Prakash, M. S. Bull, and M. Prakash, *Nat. Phys.* **17**, 504 (2021). doi:10.1038/s41567-020-01134-7
- [29] K. Grell and A. P. Ruthmann, in *Microscopic Anatomy of Invertebrates, Placozoa, Porifera, Cnidaria and Ctenophora*, edited by F. W. Harrison and J. A. Westfall (Wiley, New York, NY, 1991), p. 13.
- [30] C. L. Smith, N. Pivovarova, and T. S. Reese, *PLoS ONE* **10**, e0136098 (2015). doi:10.1371/journal.pone.0136098

- [31] G. Buzsáki and A. Draguhn, *Science* **304**, 1926 (2004). doi:10.1126/science.1099745
- [32] P. Lenz and L. Søgaard-Andersen, *Nat. Rev. Microbiol.* **9**, 565 (2011). doi:10.1038/nrmicro2612
- [33] L. Potvin-Trottier, N. D. Lord, G. Vinnicombe, and J. Paulsson, *Nature (London)* **538**, 514 (2016). doi:10.1038/nature19841
- [34] M. Guzzo, S. M. Murray, E. Martineau, S. Lhospice, G. Baronian, L. My, Y. Zhang, L. Espinosa, R. Vincentelli, B. P. Bratton, J. W. Shaevitz, V. Molle, M. Howard, and T. Mignot, *Nat. Microbiol.* **3**, 948 (2018). doi:10.1038/s41564-018-0203-x
- [35] A. Ruthmann, G. Behrendt, and R. Wahl, *Zoomorphology* **106**, 115 (1986). doi:10.1007/BF00312113
- [36] C. L. Smith, F. Varoquaux, M. Kittelmann, R. N. Azam, B. Cooper, C. A. Winters, M. Eitel, D. Fasshauer, and T. S. Reese, *Curr. Biol.* **24**, 1565 (2014). doi:10.1016/j.cub.2014.05.046
- [37] M. S. Bull, V. N. Prakash, and M. Prakash, arXiv:2107.02934 (2021).
- [38] This increase can be demonstrated by locally deforming the geometry of cellular arrangement in a specific neighborhood so as to isolate one of the receiver cells from its neighboring transmitter cells, thereby allowing it to become a transmitter cell itself (augmenting their number by unity). See Supplementary Information for details.
- [39] For movies showing the time-evolution of the dynamics in the arrays, see Supplementary Information.
- [40] J. Lewis, *Curr. Biol.* **13**, 1398 (2003). doi:10.1016/S0960-9822(03)00534-7
- [41] C. Kuyyamudi, S. N. Menon, and S. Sinha, *Phys. Biol.* **19**, 016001 (2021). doi:10.1088/1478-3975/ac31a3
- [42] W.-M. Deng, C. Althausen, and H. Ruohola-Baker, *Development* **128**, 4737 (2001). doi:10.1242/dev.128.23.4737
- [43] H. Shimojo, T. Ohtsuka, and R. Kageyama, *Neuron* **58**, 52 (2008). doi:10.1016/j.neuron.2008.02.014
- [44] M. B. Elowitz and S. Leibler, *Nature (London)* **403**, 335 (2000). doi:10.1038/35002125
- [45] R. FitzHugh, *Biophysical Journal* **1**, 445 (1961). doi:10.1016/s0006-3495(61)86902-6
- [46] J. Nagumo, S. Arimoto, and S. Yoshizawa, *Proc. IRE* **50**, 2061 (1962). doi:10.1109/jrproc.1962.288235
- [47] S. Sinha and S. Sridhar, *Patterns in Excitable Media* (CRC Press, Boca Raton, FL, 2015).
- [48] R. Singh and S. Sinha, *Phys. Rev. E* **87**, 012907 (2013). doi:10.1103/PhysRevE.87.012907
- [49] R. Janaki, S. N. Menon, R. Singh, and S. Sinha, *Phys. Rev. E* **99**, 052216 (2019). doi:10.1103/PhysRevE.99.052216
- [50] We count n_h as the number of cells having $L_{SS} > 0.2$. We have verified that the specific choice of the threshold value does not qualitatively change our results.
- [51] See Supplementary Information.
- [52] P. Heitzler and P. Simpson, *Cell* **64**, 1083 (1991). doi:10.1016/0092-8674(91)90263-X
- [53] R. Kageyama, T. Ohtsuka, H. Shimojo, and I. Imayoshi, *Nat. Neurosci.* **11**, 1247 (2008). doi:10.1038/nn.2208
- [54] S. Nonaka, Y. T. Y. Okada, S. T. A. Harada, Y. Kanai, M. Kido, and N. Hirokawa, *Cell* **95** (1998). doi:10.1016/s0092-8674(00)81705-5
- [55] V. B. Pearse and O. Voigt, *Integr. Comp. Biol.* **47**, 677 (2007). doi:10.1093/icb/icm015
- [56] A. Prindle, J. Liu, M. Asally, S. Ly, J. Garcia-Ojalvo, and G. M. Süel, *Nature (London)* **527**, 59 (2015). doi:10.1038/nature15709
- [57] J. Humphries, L. Xiong, J. Liu, A. Prindle, F. Yuan, H. A. Arjes, L. Tsimring, and G. M. Süel, *Cell* **168**, 200 (2017). doi:10.1016/j.cell.2016.12.014

SUPPLEMENTARY INFORMATION

Contact-mediated signaling enables disorder-driven transitions in cellular assemblies

Chandrashekar Kuyyamudi, Shakti N. Menon and Sitabhra Sinha

LIST OF SUPPLEMENTARY FIGURES AND MOVIES

1. Fig S1: Disordered cellular arrangement can promote cell fate choices that are constrained by lateral inhibition.
2. Fig S2: Disorder enhances fate pattern robustness against random cell damage.
3. Fig S4: Reduced variability of fate distribution with increased disorder in tissues subject to random cell damage.
4. Fig S5: Disorder promotes emergence of chimera states in diffusively coupled relaxation oscillators.
5. Fig S4: Chimera states are robust with respect to noise.
6. Movie S1: Time-evolution of C gene expression in an ordered array of repressilators interacting by contact-induced signaling.
7. Movie S2: Time-evolution of C gene expression in a disordered arrangement of repressilators interacting by contact-induced signaling.
8. Movie S3: Time-evolution of the inactivation variable y in an ordered array of diffusively coupled relaxation oscillators.
9. Movie S4: Time-evolution of the inactivation variable y in a disordered arrangement of diffusively coupled relaxation oscillators.

NUMERICAL DETAILS

The dynamics of each cell in the various models investigated here are described by systems of coupled ordinary differential equations (ODEs). We solve these coupled ODEs using an adaptive numerical integrator (implemented in the differential equations module in Julia programming language, ver. 1.6.1). The initial values of the dynamical variables have been chosen from uniform random distributions.

The steady state distributions of ligand concentrations shown in Fig. 2 (b) in the main text have been obtained by Gaussian kernel smoothing, sampling over 300 independent trials for four different values of σ_P .

In Fig. 2 (e) shown in the main text, we consider 10 different lattices and 30 different choices of damaged cells for each level of disorder (σ_P) and measure n_h for each of the trials. We quantify the robustness with respect to random cell damage by measuring the variance in n_h across 300 different realizations. From the distributions obtained after Gaussian kernel smoothing shown in Fig. S3, we observe that while the mean value of n_h increases with σ_P , the variance $[\sigma^2(n_h)]$ noticeably decreases with increase in the level of disorder in the lattice.

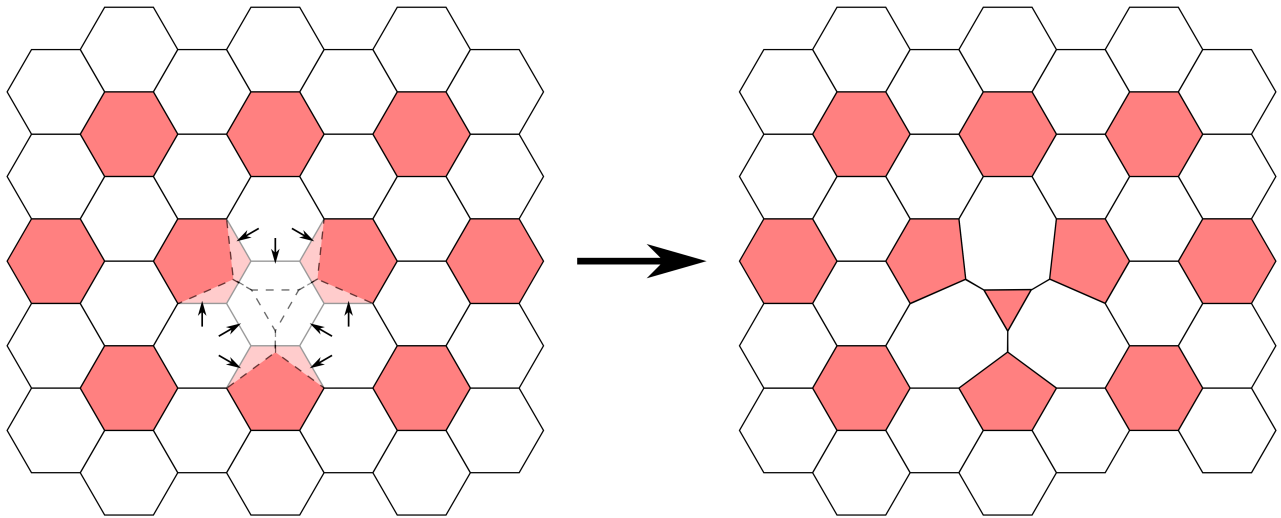


FIG. S1. Disordered cellular arrangement can promote cell fate choices that are constrained by lateral inhibition. The schematic diagrams represent a completely ordered hexagonal close-packed lattice of cells (left) that is deformed to yield the locally disordered arrangement comprising polygons that have either more or fewer than six neighbors (right). Colored polygons represent cells that have adopted a specialized fate, e.g., transmitter cells in the example discussed in the main text. This fate choice is assumed to be subject to lateral inhibition, so that adjacent cells cannot both be colored. Note that a hexagon that was in contact with three colored polygons in the ordered case becomes triangular upon deformation and is free to be colored (i.e., adopt the specialized cell fate) as it no longer neighbors any other colored cell. Thus, the number of colored cells increase by 1, even though the number of cells and the total number of cell-cell contacts are conserved.

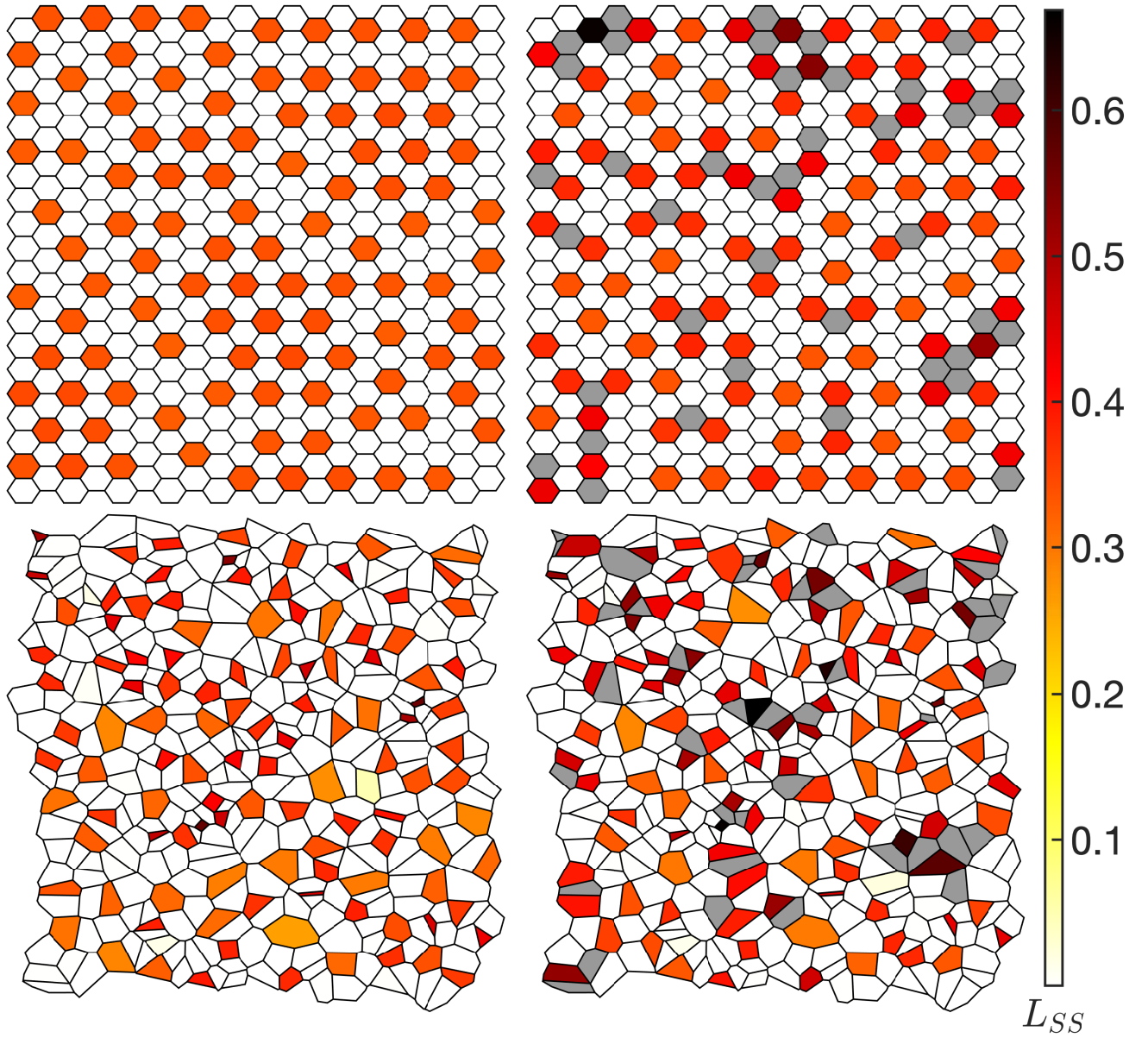


FIG. S2. **Disorder enhances fate pattern robustness against random cell damage.** The steady state spatial arrangement of cell fates in (top row) the absence of disorder ($\sigma_P = 0$) and (bottom row) with maximal disorder ($\sigma_P = 1$), comparing the situation (left) where all cells are signaling with the case (right) in which 10% of the cells (randomly chosen) are inert. The colors represent the steady state values of the Delta ligand concentration, L_{SS} . The change in the fraction of cells attaining minority fate as a consequence of disruption resulting in loss of signaling ability by part of the population, is seen to be less when the tissue is more disordered.

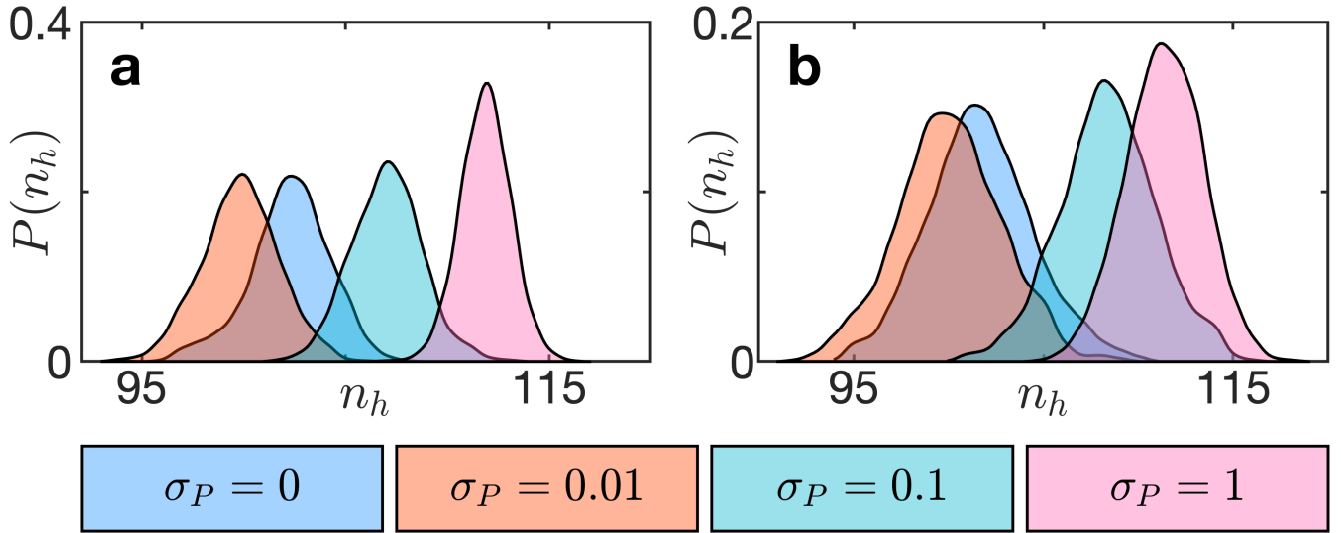


FIG. S3. **Reduced variability of fate distribution with increased disorder in tissues subject to random cell damage.** The distributions of n_h are shown for different σ_P (see key) when (a) 1% and (b) 5% of randomly chosen cells are rendered inert. We note that although the mean increases, the dispersion in n_h decreases with increasing disorder, as indicated explicitly in Fig. 2 (e) in the main text.

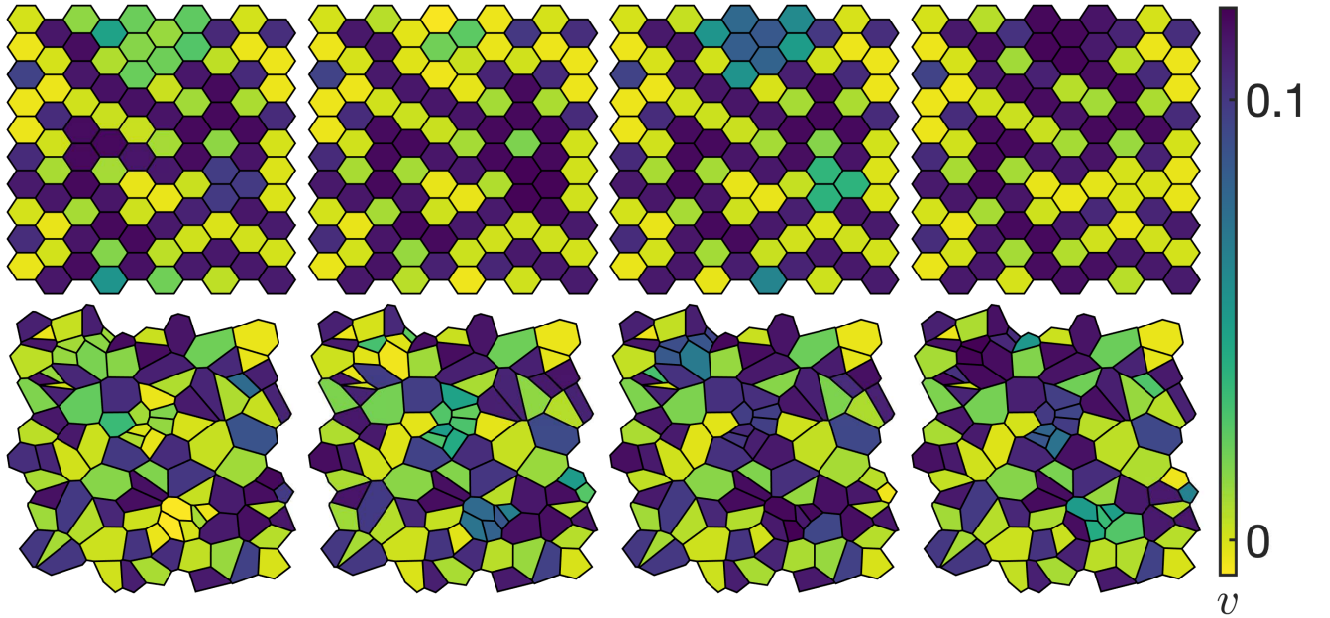


FIG. S4. **Disorder promotes emergence of chimera states in diffusively coupled relaxation oscillators.** Snapshots of (top row) an ordered lattice ($\sigma_P = 0$) and (bottom row) a maximally disordered lattice ($\sigma_P = 1$) comprising $N = 100$ relaxation oscillators shown at different times that are separated by an interval $\tau_p/4$ where τ_p is the oscillation period of an uncoupled cell. The colors represent the instantaneous value of the inactivation variable y in the Fitzhugh-Nagumo model used to describe the relaxation oscillator dynamics. Movies included in the Supplementary Information show the time-evolution of the dynamics in the arrays.

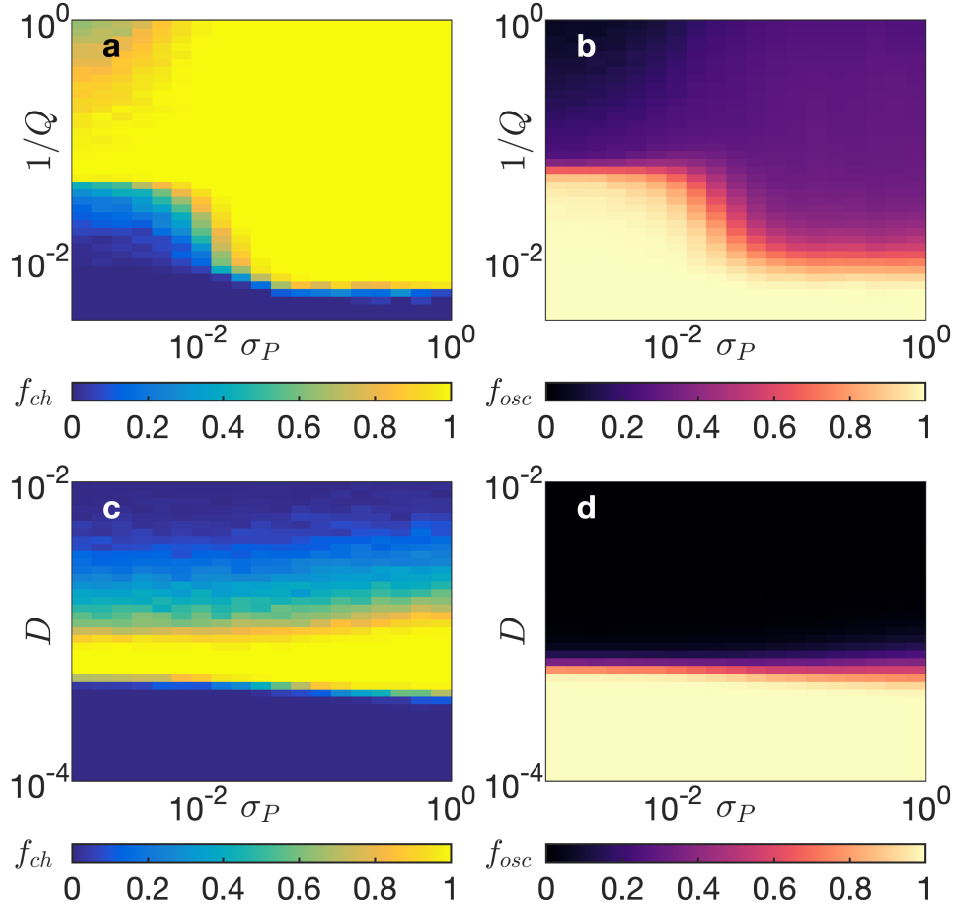


FIG. S5. **Chimera states are robust with respect to noise.** Stochastic perturbation of the intra-cellular dynamics has been implemented by adding the term $\eta \mathbf{X} dW$ to the deterministic equations $d\mathbf{X} = \mathcal{F}_{\mathbf{X}} dt$ shown in the main text ($\mathbf{X} : \{A, B, C\}$ for the repressilator, top row, and $\mathbf{X} : \{u, v\}$ for the Fitzhugh-Nagumo oscillator, bottom row). The parameter η ($= 0.01$ for the results shown here) is the strength of the noise and dW is a Wiener process. It is evident that the fraction of realizations f_{ch} in which chimera states are observed (a,c) and the mean fraction of cells that continue to oscillate f_{osc} (b,d) for the two systems subject to noise are almost identical to that in the absence of noise (shown Fig. 3 (b-e) in main text). Note that the additive stochastic term induces oscillations in the FHN model, so that larger values of D are required to arrest activity compared to the deterministic situation.